

## Complete Relative Stereochemistry of Multiple Stereocenters Using Only Residual Dipolar Couplings

Jiangli Yan,<sup>†,‡</sup> Frank Delaglio,<sup>‡</sup> Andreas Kaerner,<sup>§</sup> Allen D. Kline,<sup>†</sup> Huaping Mo,<sup>†</sup> Michael J. Shapiro,<sup>\*,†</sup> Tim A. Smitka,<sup>§</sup> Gregory A. Stephenson,<sup>§</sup> and Edward R. Zartler<sup>†</sup>

*Contribution from the Discovery Chemistry Research and Technologies, Lilly Research Labs, Lilly Corporate Center, Eli Lilly & Company, Indianapolis, Indiana 46285, Laboratory of Chemical Physics, National Institute of Diabetes and Digestive and Kidney Diseases, National Institutes of Health, Bethesda, Maryland 20892, and Pharmaceutical Product Development, Lilly Research Labs, Lilly Corporate Center, Eli Lilly & Company, Indianapolis, Indiana 46285*

Received July 29, 2003 E-mail: shapiro\_mike@lilly.com

**Abstract:** Residual dipolar couplings (RDCs), in combination with molecular order matrix calculations, were used to unambiguously determine the complete relative stereochemistry of an organic compound with five stereocenters. Three simple one-dimensional experiments were utilized for the measurements of  $^{13}\text{C}-^1\text{H}$ ,  $^{13}\text{C}-^{19}\text{F}$ ,  $^{19}\text{F}-^1\text{H}$ , and  $^1\text{H}-^1\text{H}$  RDCs. The order matrix calculation was performed on each chiral isomer independently. The fits were evaluated by the comparison of the root-mean-square deviation (rmsd) of calculated and measured RDCs. The order tensor simulations based on two different sets of RDC data collected with phage and bicelles are consistent. The resulting stereochemical assignments of the stereocenters obtained from using only RDCs are in perfect agreement with those obtained from the single-crystal X-ray structure. Six RDCs are found to be necessary to run the simulation, and seven are the minimum to get an acceptable result for the investigated compound. It was also shown that  $^{13}\text{C}-^1\text{H}$  and  $^1\text{H}-^1\text{H}$  RDCs, which are the easiest to measure, are also the most important and information-rich data for the order matrix calculation. The effect of each RDC on the calculation depends on the location of the corresponding vector in the structure. The direct RDC of a stereocenter is important to the configuration determination, but the configuration of stereocenters devoid of protons can also be obtained from analysis of nearby RDCs.

### Introduction

The determination of stereochemistry of organic molecules represents a major effort in medicinal chemistry. It is the most crucial part of the characterization of unknown compounds, both of synthetic and natural products, especially those with biological activities. When single crystals are available, X-ray crystallographic analysis can determine the stereochemistry relative to a stereocenter of known stereochemistry, or the absolute stereochemistry may be determined directly if a heavy atom, typically S or heavier, is present in the structure.<sup>1,2</sup> Nuclear magnetic resonance (NMR) spectroscopy is another approach to address this kind of problem. Solution NMR plays an important role for those compounds not forming adequate crystals for X-ray diffraction analysis. Stereochemistry by NMR spectroscopy for most organic molecules is typically accomplished using a combination of nuclear Overhauser effect

(NOE) and short-range or long-range scalar  $J$  couplings.<sup>3</sup> The analysis of stereochemistry by NOE and homonuclear  $J$  coupling analysis depends on "proton bridges". Protons less than 5 Å apart are used in a NOE walk. The measurement of  $^3J_{\text{HH}}$  couplings leads to estimates of the dihedral angles through the well-known Karplus equation<sup>4</sup> and the relative orientations by sequential connectivity. The measurement of long-range heteronuclear  $J$  couplings ( $\geq ^2J_{\text{XH}}$ ) are also useful but not always favorable when the sample is not  $^{13}\text{C}$  enriched, since the experiments, such as heteronuclear multiple bond coherence spectroscopy (HMBC),<sup>5,6</sup> can be time-consuming. If the molecule of interest has an overall dearth of protons or some NOEs that cannot be unambiguously assigned, the NOE and  $J$  analysis fail. Additionally, to get the relative orientation of remote centers, multiple NOE or  $J$ -coupling connections have to be performed in series to transverse the entire molecule. The further the stereocenters are from each other, the greater the number of necessary connections and measurements that are needed to make connectivity. If one of the connections fails, the pathway

<sup>†</sup> Discovery Chemistry Research and Technologies, Eli Lilly & Company.

<sup>‡</sup> Present address: Triad Therapeutics, Inc., 9381 Judicial Dr., Suite 200, San Diego, CA 92121.

<sup>§</sup> National Institutes of Health.

<sup>\*</sup> Pharmaceutical Product Development, Eli Lilly & Company.

(1) Flack, H. D.; Bernardinelli, G. *Acta Crystallogr., Sect. A* **1999**, *A55*, 908–915.

(2) Flack, H. D.; Bernardinelli, G. *J. Appl. Crystallogr.* **2000**, *33*, 1143–1148.

(3) Neri, P.; Tringali, C. *Bioact. Compd. Nat. Sources* **2001**, 69–127.

(4) Karplus, M. *J. Am. Chem. Soc.* **1963**, *85*, 2870–2871.

(5) Summers, M. F.; Marzilli, G. L.; Bax, A. *J. Am. Chem. Soc.* **1986**, *108*, 4285–4294.

(6) Bax, A.; Subramanian, S. *J. Magn. Reson.* **1986**, *67*, 565–569.

fails. Therefore, the development of new methodology to circumvent this problem is desired.

Residual dipolar coupling (RDC) is another structural information-rich NMR parameter. RDCs were first measured in solution by NMR in the 1960s.<sup>7</sup> These early studies focused on organic liquid crystals and produced very large dipolar couplings, which proved difficult to analyze. Subsequent studies, by many groups, notably Bothner-By's, used the molecule's magnetic susceptibility anisotropy (diamagnetic at first, later paramagnetic) yielding a smaller degree of alignment and smaller couplings.<sup>8–10</sup> The RDCs observed in these studies were used to get structural information of small magnetically anisotropic molecules. In the past decade, RDCs have been measured for biomolecules partially aligned by liquid crystals.<sup>11–16</sup> RDCs have been widely utilized in the structural determination of proteins,<sup>17</sup> nucleic acids,<sup>18</sup> and biopolymers<sup>16</sup> and for studying molecular dynamics.<sup>19</sup>

Residual dipolar coupling between two directly coupled nuclei A and B can be described by eq 1 in the molecular frame:<sup>20–22</sup>

$$D^{\text{AB}}(\theta, \phi) = -\frac{\mu_0 h}{16\pi^3} \gamma_A \gamma_B \left\{ D_a^{\text{AB}} (3 \cos^2 \theta - 1) + \frac{3}{2} D_r^{\text{AB}} (\sin^2 \theta \cos 2\phi) \right\} S A_a \langle r_{\text{AB}}^{-3} \rangle \quad (1)$$

where  $\theta$  denotes the fixed polar angle between the A–B interatomic vector and the  $z$  axis of the order tensor;  $\phi$  is the angle that describes the position of the projection of the A–B interatomic vector on the  $x$ – $y$  plane, relative to the  $x$  axis;  $\gamma_A$  and  $\gamma_B$  are the gyromagnetic ratios of each interacting nucleus;  $D_a^{\text{AB}}$  and  $D_r^{\text{AB}}$  in units of Hz are the axial and rhombic components of the order tensor;  $A_a$  is the unitless axial component of the molecular alignment tensor;  $S$  is the generalized order parameter;  $r_{\text{AB}}$  is the A–B distance; and the  $\langle \rangle$  brackets indicate motional averaging due to molecular tumbling. The power of RDCs is that the angular terms of eq 1 can be exploited for structural studies. The distance dependence of RDCs is  $r^{-3}$  (vs  $r^{-6}$  for NOE) and therefore allows longer-range internuclear interactions to be monitored. RDCs are not limited to  $^1\text{H}$ – $^1\text{H}$  interactions and can also be monitored for a wide range of nuclei, e.g.,  $^1\text{H}$ – $^{13}\text{C}$ ,  $^{13}\text{C}$ – $^{15}\text{N}$ ,  $^1\text{H}$ – $^{15}\text{N}$ , etc., and thus can provide a wider range of structural information than  $^1\text{H}$ – $^1\text{H}$  NOEs.

In order matrix analysis, RDCs are used to determine the five independent elements of a symmetric and traceless  $3 \times 3$

order matrix.<sup>23,24</sup> The axial and rhombic components  $D_a$  and  $D_r$  as well as Euler angles  $\alpha$ ,  $\beta$ , and  $\gamma$  are used to describe the molecular orientation relative to the laboratory frame. These five parameters can be therefore reformulated in terms of an alignment of axes (three angles) for a principle order frame and values of principal order parameters ( $S_{zz}$ ,  $S_{yy}$ , and  $S_{xx}$ ) by<sup>25</sup>

$$S_{zz} = \frac{2}{k} D_a; S_{yy} = -\frac{1}{k} D_a \left( 1 + \frac{3}{2} R \right); S_{xx} = -\frac{1}{k} D_a \left( 1 - \frac{3}{2} R \right) \quad (2)$$

where  $k = (-2\mu_0 h / 16\pi^3) \gamma_A \gamma_B (1/r_{\text{AB}}^3)$  and  $R = (D_r/D_a)$ . With a known molecular order tensor, the RDC of any vector can be predicted from a given structure. Fits are usually evaluated using the root-mean-square-deviation (rmsd) of calculated and measured RDC.

$$\text{rmsd} = \left( \sum_n w (D_{\text{calc}} - D_{\text{exp}})^2 / n \right)^{1/2} \quad (3)$$

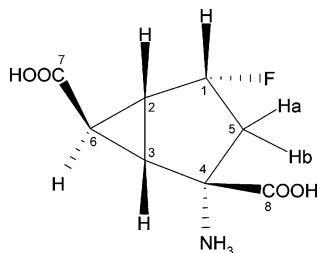
An asymmetry parameter  $\eta$  ( $= |(S_{xx} - S_{yy})/S_{zz}|$ ) can also be derived to study the molecular motion.<sup>23,24,26</sup>

Despite the blossoming use of RDCs in biological systems, the utility of this technique for organic molecule structure determination has not been explored extensively. Recently, some carbohydrate structures have been studied using RDC.<sup>27–31</sup> Methods for the RDC measurements of small molecules have been developed.<sup>27,32</sup> In fact, any methodology that is able to measure  $J$  couplings can be utilized to measure RDCs. Since RDCs are typically small (generally in the range of  $-20$  to  $+20$  Hz), precision is critical. Measurement in the direct dimension has the most resolution and therefore has the advantage over indirect measurement for this reason. It is vital that couplings that are only first-order be used in this way. Non-first-order couplings should only be used with great care.

In addition to water-soluble alignment media, such as bacteria phage<sup>33–36</sup> and bicelles,<sup>15,37,38</sup> many efforts are focused on nonaqueous liquid crystals.<sup>39–42</sup> One example is the work reported by Bendiak, where deuterated PCBP (4-*n*-pentyl-4'-cyanobiphenyl) was used as a solvent and as an orientation medium for a small organic compound. Thus, this method is usable in aqueous and nonaqueous media.

- (7) Saupe, A.; Englert, G. *Phys. Rev. Lett.* **1963**, *11*, 462–464.
- (8) Lohman, J. A. B.; MacLean, C. *Chem. Phys.* **1978**, *35*, 269–274.
- (9) Bothner-By, A. A.; Domaille, P. J.; Gayathri, C. *J. Am. Chem. Soc.* **1981**, *103*, 5602–5603.
- (10) Lisicki, M. A.; Mishra, P. K.; Bothner-By, A. A.; Lindsey, J. S. *J. Phys. Chem.* **1988**, *92*, 3400–3403.
- (11) Ram, P.; Prestegard, J. H. *Biochim. Biophys. Acta* **1988**, *940*, 289–294.
- (12) Sanders, C. R., II; Prestegard, J. H. *Biophys. J.* **1990**, *58*, 447–460.
- (13) Tolman, J. R.; Flanagan, J. M.; Kennedy, M. A.; Prestegard, J. H. *Proc. Natl. Acad. Sci. U.S.A.* **1995**, *92*, 9279–9283.
- (14) Tjandra, N.; Grzesiek, S.; Bax, A. *J. Am. Chem. Soc.* **1996**, *118*, 6264–6272.
- (15) Tjandra, N.; Bax, A. *J. Magn. Reson.* **1997**, *124*, 512–515.
- (16) de Alba, E.; Tjandra, N. *Prog. Nucl. Magn. Reson.* **2002**, *40*, 175–197.
- (17) Brunner, E. *Concepts Magn. Reson.* **2001**, *13*, 238–259.
- (18) MacDonald, D.; Lu, P. *Curr. Opin. Struct. Biol.* **2002**, *12*, 337–343.
- (19) Tolman, J. R. *Curr. Opin. Struct. Biol.* **2001**, *11*, 531–539.
- (20) Clore, G. M.; Gronenborn, A. M. *Proc. Natl. Acad. Sci. U.S.A.* **1998**, *95*, 5891–5898.
- (21) Clore, G. M.; Gronenborn, A. M.; Bax, A. *J. Magn. Reson.* **1998**, *133*, 216–221.
- (22) Bax, A.; Tjandra, N. *J. Biol. NMR* **1997**, *10*, 289–292.

- (23) Saupe, A. *Angew. Chem., Int. Ed. Engl.* **1968**, *7*, 97–112.
- (24) Losonczi, J. A.; Andrec, M.; Fischer, M. W. F.; Prestegard, J. H. *J. Magn. Reson.* **1999**, *138*, 334–342.
- (25) Fischer, M. W. F.; Losonczi, J. A.; Weaver, J. L.; Prestegard, J. H. *Biochemistry* **1999**, *38*, 9013–9022.
- (26) Al-Hashimi, H. M.; Valafar, H.; Terrell, M.; Zartler, E. R.; Eidsness, M. K.; Prestegard, J. H. *J. Magn. Reson.* **2000**, *143*, 402.
- (27) Yan, J.; Kline, A. D.; Mo, H.; Shapiro, M. J.; Zartler, E. R. *J. Org. Chem.* **2003**, *68*, 1786–1795.
- (28) Neubauer, H.; Meiler, J.; Peti, W.; Griesinger, C. *Helv. Chim. Acta* **2001**, *84*, 243–258.
- (29) Freedberg, D. I. *J. Am. Chem. Soc.* **2002**, *124*, 2358–2362.
- (30) Azurmendi, H. F.; Bush, C. A. *Carbohydr. Res.* **2002**, *337*, 905–915.
- (31) Martin-Pastor, M.; Bush, C. A. *Biochemistry* **2000**, *39*, 4674–4683.
- (32) Thiele, C. M.; Berger, S. *Org. Lett.* **2003**, *5*, 705–708.
- (33) Hansen, M. R.; Mueller, L.; Pardi, A. *Nat. Struct. Biol.* **1998**, *5*, 1065–1074.
- (34) Trempe, J.-F.; Morin, F. G.; Xia, Z.; Marchessault, R. H.; Gehring, K. J. *Biomol. NMR* **2002**, *22*, 83–87.
- (35) Zweckstetter, M.; Bax, A. *J. Biol. NMR* **2001**, *20*, 365–377.
- (36) Barrientos, L. G.; Louis, J. M.; Gronenborn, A. M. *J. Magn. Reson.* **2001**, *149*, 154–158.
- (37) Ottiger, M.; Bax, A. *J. Biol. NMR* **1998**, *12*, 361–372.
- (38) Losonczi, J. A.; Prestegard, J. H. *J. Biol. NMR* **1998**, *12*, 447–451.
- (39) Sarfati, M.; Courtieu, J.; Lesot, P. *Chem. Commun.* **2000**, 1113–1114.
- (40) Sarfati, M.; Lesot, P.; Merlet, D.; Courtieu, J. *Chem. Commun.* **2000**, 2069–2081.
- (41) Aroulanda, C.; Sarfati, M.; Courtieu, J.; Lesot, P. *Enantiomer* **2001**, *6*, 281–287.
- (42) Bendiak, B. *J. Am. Chem. Soc.* **2002**, *124*, 14862–14863.

**Scheme 1.** Structure of Compound **1**<sup>a</sup>

<sup>a</sup>Atom ID of each carbon is indicated.

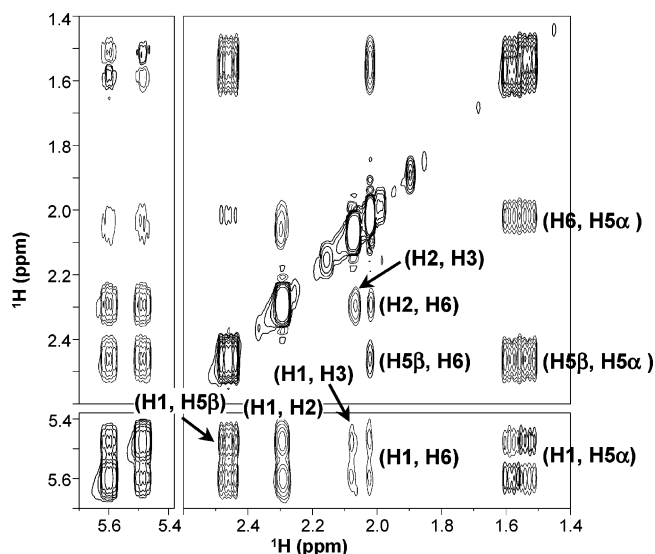
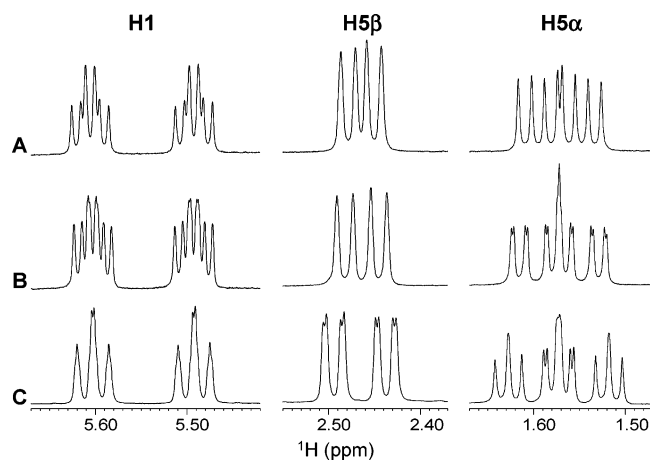
**Table 1.** <sup>1</sup>H and <sup>13</sup>C Chemical Shifts of Fused-Ring Atoms of Compound **1** Shown in Scheme 1 (data collected at 25 °C)

position	<sup>1</sup> H chemical shift (ppm)	<sup>13</sup> C chemical shift (ppm)
1	5.54	94.4
2	2.28	30.5
3	2.07	32.2
4		65.1
5 $\alpha$	1.57	35.6
5 $\beta$	2.45	
6	2.02	22.4

We recently reported a novel method to study the remote relative stereochemistry of six-membered chairlike ring compounds based on the simple inspection of <sup>13</sup>C–<sup>1</sup>H RDCs without further calculation of the order tensor.<sup>27</sup> In this current paper, we performed a complete order matrix calculation to determine the complete stereochemistry of an organic compound (compound **1**) containing five stereocenters. Homo- and heteronuclear RDCs were measured from three one-dimensional experiments. 1D heteronuclear multiple quantum coherence (HMQC)<sup>27,43</sup> was used for <sup>13</sup>C–<sup>1</sup>H RDCs; 1D NOE enhanced <sup>13</sup>C experiment was used for <sup>13</sup>C–<sup>19</sup>F RDCs; a few <sup>19</sup>F–<sup>1</sup>H and <sup>1</sup>H–<sup>1</sup>H RDCs were accurately measured by a 1D <sup>1</sup>H experiment. The order matrix calculation was performed for each of the potential chiral isomers, and the complete relative stereochemistry of compound **1** was unambiguously determined by analyzing the output data. The order tensor calculation was accomplished independently for two sets of RDC data obtained with phage and bicelles, and the results were consistent.

## Results and Discussion

Compound **1**<sup>44</sup> shown in Scheme 1 is a model compound with five stereocenters designated C1, C2, C3, C4, and C6. The proton and carbon chemical shifts were assigned on the basis of 1D <sup>1</sup>H and <sup>13</sup>C, 2D HMQC, and COSY experiments and are listed in Table 1. On the basis of the number of stereocenters this compound has 32 potential isomers. Since it is impossible to have a *trans* configuration between H2 and H3 at the adjacent centers of the ring juncture, the number of potential isomers is reduced to 16. The key structural question for this compound, like many other organic compounds, is the determination of its stereochemistry. Typically, the relative stereochemistry of this kind of molecule would be solved by NOE and *J* coupling analysis. The 2D NOESY spectrum and assignments for compound **1** are shown in Figure 1. It is clear from Figure 1 that H6 and H5 $\alpha$  are on the same side of the fused ring. But the stereochemistry of H6 relative to H2/H3 is ambiguous

**Figure 1.** 2D NOESY spectrum of 10 mM compound **1** in PBS buffer (pD 7.1) recorded at 25 °C. A mixing time of 1.2 s was used, while the recovery time was 2 s. A total of 1024(*t*<sub>2</sub>) × 256(*t*<sub>1</sub>) data points were recorded to cover 4808 Hz in each dimension. NOE assignments are presented.**Figure 2.** (A) Expanded proton spectrum of 10 mM compound **1** in PBS buffer (pD 7.1). The experiment was performed at 25 °C. (B) Expanded proton spectrum of 10 mM compound **1** in PBS buffer containing 15 mg/mL phage (pD 7.1). The experiment was performed at 25 °C. (C) Expanded proton spectrum of 10 mM compound **1** in PBS buffer containing 10% bicelles (pD 6.3). The experiment was performed at 31 °C. Other experimental condition for A, B, and C were identical. A total of 32k data points were acquired to digitize 4808 Hz and resulted in a FID resolution of 0.12 Hz.

because the distances from H6 to H2/H3 are similar in both the *trans* (3.2 Å) and *cis* (2.5 Å) configurations, while H5 $\alpha$  and H5 $\beta$  are too far from H2/H3 to build up NOEs. For the same reason, the relative stereochemistry of H1 to H2 and H1 to H5 $\alpha$  or H5 $\beta$  cannot be determined unambiguously. Thus, the NOE experiment is unable to solve the complete relative stereochemistry of this simple compound in this case. The three-bond, four-bond, or even longer-range H–H *J* couplings might help in this case if the Karplus equations of this kind of fused-ring molecule are known.

**Measurement of RDC.** The <sup>1</sup>H spectra of compound **1**, shown in Figure 2, indicate that both pf1 phage (15 mg/mL) and bicelles (10%; DMPC:DHPC is 2.8:1) can orient this compound, but bicelles give a larger degree of alignment. The RDC data were collected using three simple 1D experiments.

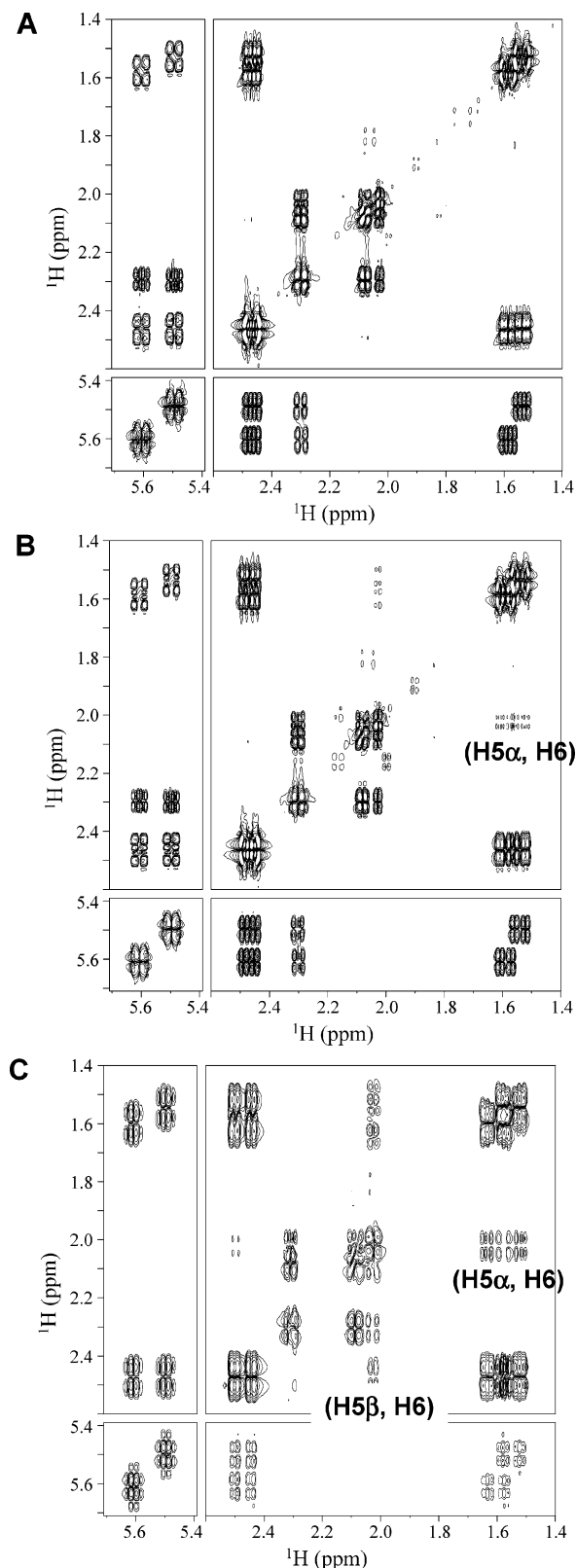
(43) Bax, A.; Griffey, R. H.; Hawkins, B. L. *J. Magn. Reson.* **1983**, *55*, 301–315.

(44) Massey, S. M.; Monn, J. A.; Valli, M. J. *Eur. Pat. Appl.* 1998, 35 pp.



Six  $^{13}\text{C}$ – $^1\text{H}$  RDCs were determined from the 1D HMQC experiment.<sup>27,43</sup>  $J$  and  $J + \text{RDC}$  of each  $^{13}\text{C}$ – $^1\text{H}$  group were measured by the frequency difference of two  $^{13}\text{C}$  satellites. To correct the phase distortion observed in direct measurement of HMQC,<sup>15</sup> each of the  $^{13}\text{C}$  satellites was phased independently before the signal frequencies were recorded.<sup>27</sup> A 1D NOE-enhanced, proton-decoupled  $^{13}\text{C}$  experiment allowed six  $^{13}\text{C}$ – $^{19}\text{F}$  RDCs to be detected. Two  $^{19}\text{F}$ – $^1\text{H}$  and three or four (depending on the alignment media)  $^1\text{H}$ – $^1\text{H}$  RDCs could be measured accurately from the 1D  $^1\text{H}$  spectra. In principle, more than four  $^1\text{H}$ – $^1\text{H}$  couplings can be observed in  $^1\text{H}$  experiments for this compound; however only the signals of H1, H5 $\alpha$ , and H5 $\beta$  (as shown in Figure 2) were utilized for the measurements, since the coupling patterns of these signals are clear, while the others have very complex coupling patterns. From the H1 signal, the two-bond  $J$  and RDC of F–H1 were measured. When the compound was aligned by phage, an additional dipolar coupling was observed between H5 $\alpha$  and H6, which cannot be detected in the isotropic phase. Analysis of the coupling interactions to H5 $\alpha$  revealed three  $^1\text{H}$ – $^1\text{H}$  RDCs (H1–H5 $\alpha$ , H5 $\alpha$ –H5 $\beta$ , and H5 $\alpha$ –H6) and one  $^{19}\text{F}$ – $^1\text{H}$  RDC (F–H5 $\alpha$ ). In addition to the RDC of H1–H5 $\alpha$ , the RDC of H5 $\alpha$ –H5 $\beta$  was also determined from the signal of H5 $\beta$ . The  $J$  and  $J + \text{RDC}$  values of H5 $\alpha$ –H5 $\beta$  measured from two signals are the same within the experimental error range. The assignment of H5 $\alpha$ –H6 RDC was accomplished by 2D DQF-COSY, as shown in Figure 3A,B. In addition to the two-bond coupling of H5 $\alpha$ –H5 $\beta$  and three-bond couplings of H5 $\alpha$ –H1 and H5 $\alpha$ –F, a pair of weak cross-peaks between H5 $\alpha$  and H6, which did not appear in the isotropic spectrum (Figure 3A), were observed (Figure 3B). This indicates a through-space long-range dipole–dipole interaction (RDC) between these two nuclei when the compound is aligned by phage. When bicelles were used as the alignment medium, the dipole–dipole interaction of H5 $\beta$ –H6 was also observed (Figure 3C), in addition to the strong through-space interaction of H5 $\alpha$ –H6. Therefore RDCs of H1–H5 $\beta$ , H5 $\alpha$ –H5 $\beta$ , and H5 $\beta$ –H6 were collected from the signal of H5 $\beta$ , while an additional RDC of H5 $\beta$ –F was measured from the resonance of H5 $\alpha$ . The H1–H5 $\alpha$  and H5 $\alpha$ –H6 RDCs could not be obtained accurately since the coupling patterns could not be identified from the 1D proton spectrum, even under aligned conditions (Figure 2C). DQF-COSY was also used to assist the assignments of other  $J$  and RDC data. All of the measured  $J$  scalar and residual dipolar couplings are listed in Table 2, with the  $J$  couplings being an average of five measurements from two different samples. The measurement deviations are smaller than the experimental FID resolution. The consistency of the data recorded with the isotropic sample and the bicelle sample at 25 °C indicates the accuracy of all the measurements. The determination of the sign of C–F, F–H, and long-range H–H  $J$  constants will be described elsewhere (manuscript in preparation).

**Determination of Relative Stereochemistry of Compound 1 Using RDC Only.** The atomic coordinates of all 16 chiral isomers of compound **1** (Scheme 1) were built atom-by-atom and energy-minimized before calculation. In the input RDC table, all RDC measurement-related atoms, except of H5 $\alpha$  and H5 $\beta$ , have a one-to-one relationship to the atomic coordinates of the initial structure. H5 $\alpha$  was defined a priori as the proton that is on the same side of H6 on the fused ring, because a

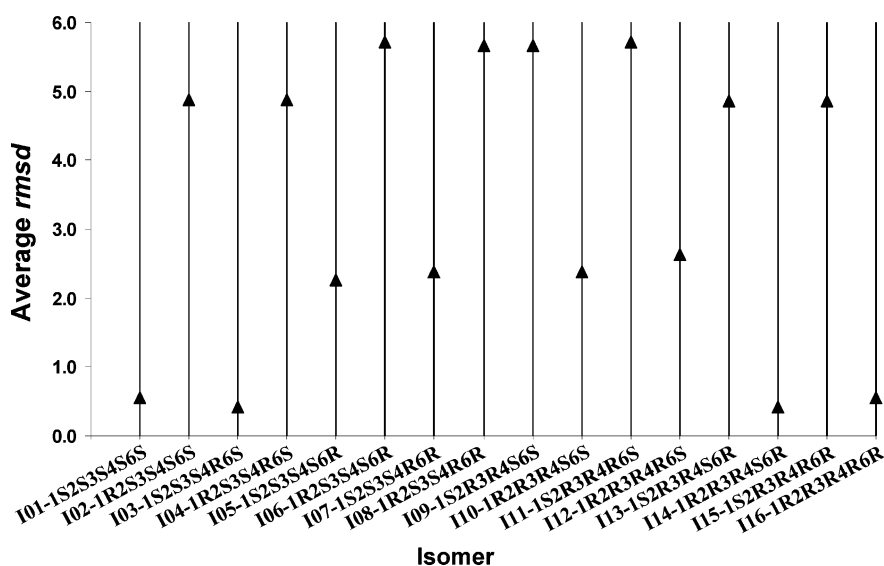


**Figure 3.** (A) 2D DQF-COSY spectrum of 10 mM compound **1** in PBS buffer (pH 7.1). The experiment was performed at 25 °C. (B) 2D DQF-COSY spectrum of 10 mM compound **1** in PBS buffer containing 15 mg/mL phage (pH 7.1). The experiment was performed at 25 °C. (C) 2D DQF-COSY spectrum of 10 mM compound **1** in PBS buffer containing 10% bicelles (pH 6.3). The experiment was performed at 31 °C. Other experimental condition for A, B, and C were identical. 256 × 1024 data points were used in both  $F_1$  and  $F_2$  dimensions with a sweep width of 4006 Hz (8.0 ppm). Quadrature indirect detection was achieved through TPPI. The recovery delay was 2 s.

**Table 2.** *J*-Scalar Couplings and Residual Dipolar Couplings Measured Using 15 mg/mL Phage and 10% Bicelles as the Alignment Media (all data are in Hz)

vector	isotropic		aligned by the phage				aligned by the bicelles			
	<i>J</i>	error <sup>a</sup>	<i>J</i> +RDC	error <sup>b</sup>	RDC	error <sup>c</sup>	<i>J</i> +RDC	error <sup>d</sup>	RDC	error <sup>e</sup>
C1–H1	162.46	0.02	160.24	0.00	–2.22	0.03	155.09	0.07	–7.37	0.09
C2–H2	177.80	0.06	179.89	0.13	2.09	0.19	182.53	0.12	4.73	0.18
C3–H3	177.18	0.01	179.38	0.03	2.20	0.04	187.53	0.42	10.35	0.43
C5–H5 $\alpha$	128.32	0.12	126.62	0.04	–1.69	0.16	127.49	0.10	–0.82	0.22
C5–H5 $\beta$	139.35	0.12	135.96	0.22	–3.39	0.33	123.89	0.22	–15.46	0.33
C6–H6	166.43	0.02	167.46	0.07	1.03	0.09	173.30	0.15	6.87	0.17
C1–F	–179.02	0.09	–178.62	0.12	0.40	0.21	–174.63	0.06	4.39	0.15
C2–F <sup>f</sup>	23.62	0.02	23.75	0.01	0.16	0.03	24.64	0.10	1.04	0.12
C3–F <sup>f</sup>	8.54	0.10	8.76	0.14	0.22	0.24	8.93	0.12	0.39	0.23
C4–F <sup>f</sup>	2.68	0.03	2.85	0.02	0.17	0.04	2.99	0.03	0.31	0.06
C5–F <sup>f</sup>	24.38	0.19	24.29	0.29	–0.09	0.48	24.92	0.18	0.54	0.37
C6–F <sup>f</sup>	3.34	0.11	3.49	0.11	0.15	0.22	3.71	0.09	0.37	0.20
F–H1	56.69	0.01	55.21	0.10	–1.48	0.11	55.23	0.00	–1.46	0.01
F–H5 $\alpha$	23.73	0.01	24.82	0.00	1.09	0.02	26.53	0.01	2.80	0.02
H1–H5 $\alpha$	7.14	0.00	7.35	0.01	0.21	0.01				
H1–H5 $\beta$	7.77	0.02	8.58	0.00	0.81	0.03	9.28	0.00	1.51	0.02
H5 $\alpha$ –H5 $\beta$	–14.25	0.02	–18.60	0.02	–4.35	0.04	–28.52	0.04	–14.27	0.05
H5 $\alpha$ –H6 <sup>f</sup>	0	0	–0.99	0.03	–0.99	0.03				
H5 $\beta$ –H6 <sup>f</sup>	0	0					–1.57	0.02	–1.57	0.03

<sup>a</sup> Measurement error is the rmsd of five repeated measurements. Three of them were performed on the regular isotropic sample at 25 °C; the others were collected on the bicelle sample at the same temperature. <sup>b</sup> Measurement error is the sum of rmsd of three measurements using the sample aligned by 15 mg/mL phage at 25 °C. <sup>c</sup> RDC measurement error is the sum of rmsd's described in a and b. <sup>d</sup> Measurement error is the sum of rmsd of two measurements using the sample aligned by 10% bicelles at 31 °C. <sup>e</sup> RDC measurement error is the sum of rmsd's described in a and d. <sup>f</sup> The determination of the sign of all long-range ( $\geq$ two-bond) C–F and five-bond H–H *J* coupling constants will be described in an upcoming publication.

**Figure 4.** Plot of the average rmsd of calculated and measured RDCs vs isomer. Calculation was performed with 17 measured RDCs, as listed in Table 2.

strong NOE between H5 $\alpha$  and H6 was observed in the NOESY spectrum (Figure 1). The input RDCs were scaled by a factor *w*, which was determined on the basis of the measurement uncertainty. If the measurement error is smaller than 2 times the digital FID resolution, then the corresponding RDC was fully weighted and *w* = 1; otherwise, *w* = 0.5. On the basis of the input RDC table (experimental data) and input structure, a molecular order tensor was then obtained for the structure by solving the molecular order matrix.<sup>24</sup> With the orientation tensor, the RDC of any vector in the molecule can be calculated from the structure. The root mean square deviation (rmsd) of the calculated RDCs to the experimental data, as described by eq 2, is utilized to assess the order tensor. If the rmsd is small on the scale of the measured RDCs, e.g., <15% of the average value of RDCs, the calculated order tensor indicates the orientation of the molecule in the laboratory frame. If the rmsd

is large on the scale of measured RDC data, it means that during the order matrix calculation no order tensor can be found for the input structure based on the input RDCs.

The calculation was performed for all 16 isomers of compound **1**, and the rmsd values are presented by a plot of average rmsd versus isomer in Figure 4 for the bicelle sample. All isomers are listed on the *x* axis in the order of the last isomer (isomer 16) being the enantiomer of the first one (isomer 1), the second to last isomer (isomer 15) being the enantiomer of the second (isomer 2), and so on. It was found that the rmsd values of two enantiomers are approximately the same. For example, both isomer **1** (all *S* configurations) and its enantiomer, isomer 16 (all *R*), have an rmsd of 0.55. There is a mirror image between isomer 1  $\rightarrow$  8 and isomer 9  $\rightarrow$  16. The rmsd of predicted RDC and experimental RDC divides the 16 isomers shown in Figure 4 into three tiers. Isomers in the lower tier

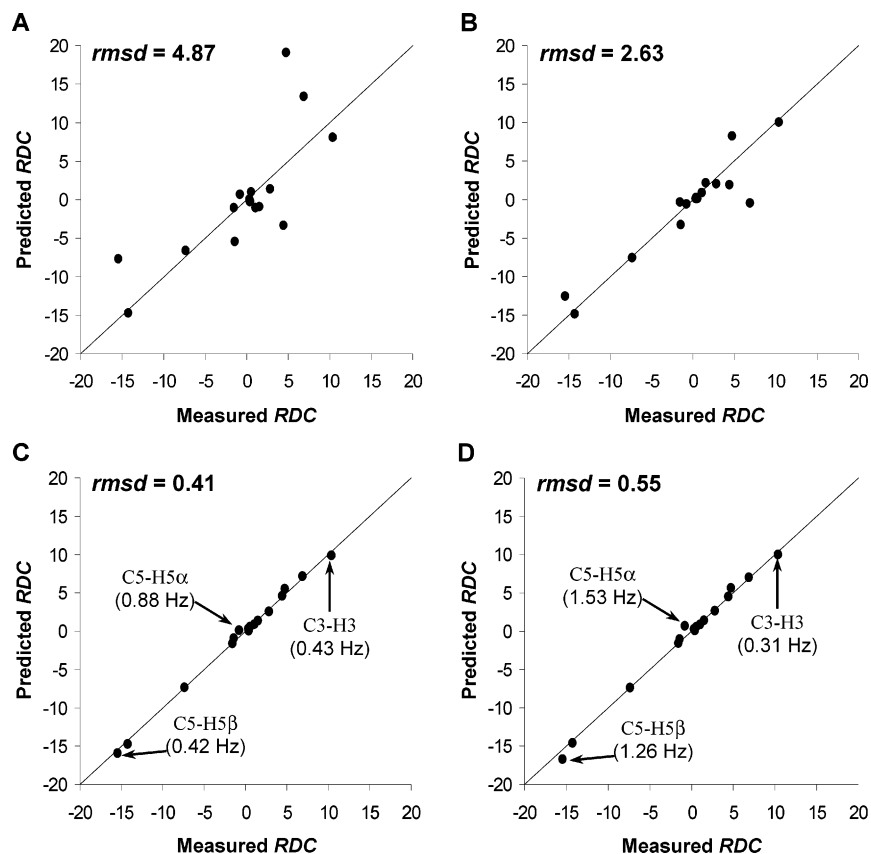


**Figure 5.** Plots of calculated RDC vs measured RDC of isomer 13 (I13-1S2R3R4S6R, A), isomer 12 (I12-1R2R3R4R6S, B), isomer 14 (I14-1R2R3R4S6R, C), and isomer 16 (I16-1R2R3R4R6R, C) of compound **1**. The rmsd value of each isomer is shown. The C–H vectors adjacent to C4 are indicated in C and D. The data in parentheses are the deviations of calculated and measured RDCs for the corresponding vector.

(isomer 1, 3, 14, and 16) have a small rmsd ( $\sim 0.5$ ). Four isomers (5, 7, 10, and 12) are located in the middle tier, and their rmsd's are 2.39 and 2.26, respectively. The rmsd's of the other eight isomers (2, 4, 6, 8, 9, 11, 13, and 15) in the upper tier are larger than 4.86. Some examples are displayed in the plots of calculated RDC versus measured RDC (Figure 5). Isomer 13 in the upper, isomer 12 in the middle, and isomer 14 and isomer 16 in the lower tier are shown in Figure 5A–D, respectively. The calculated RDCs of isomers in the upper and the middle tiers were considered inconsistent with the experimental data. The order tensor calculation found matching order tensors only for the structures in the lower tier based on the measured RDCs. Therefore the average rmsd narrows the consideration of structure from 16 isomers to the four isomers in the lower tier. The remaining four are two pairs of enantiomers (isomers 14 and 3, and 16 and 1), which are epimeric at C4.

The rmsd's of isomer 14 and isomer 16 are 0.41 and 0.55 Hz, respectively. Isomer 14 has smaller rmsd than its C4 diastereomer (isomer 16), but the rmsd difference (0.14 Hz) alone is not sufficient to distinguish them because the average deviation for RDC measurements is 0.16 Hz (Table 2). The same phenomenon was observed when isomer 3 and isomer 1 were analyzed. In fact, the compound has eight pairs of C4-diastereomers (isomer 1 and 3, 2 and 4, 5 and 7, 6 and 8, 9 and 11, 10 and 12, 13 and 15, and 14 and 16), and every pair of them have similar rmsd values. The reason for this ambiguity is that no proton exists on this center, and as a result, the only direct RDC information related to this center is a small three-bond F–C4 RDC ( $0.31 \pm 0.06$  Hz). On the other hand, the overall rmsd takes into account the entire molecule rather than

focusing on the center of interest, and therefore using the overall rmsd difference it is difficult to select between two isomers that differ by only one stereocenter. For example, in comparing isomers 14 and 16, an rmsd difference of 0.14 Hz does not reflect the real difference at only the critical center because the rmsd shown here is the total rmsd of more than 2 Hz averaged over 17 points. By analyzing the data pointwise, it can be seen that the small difference of 0.14 Hz is not contributed to equally by all points but dominated by a couple of key points, as indicated by Figure 5C,D. The biggest differences are found on the C5–H5 $\alpha$  and C5–H5 $\beta$  vectors. It would be expected that the vectors that are most sensitive to the configuration of the C4 center should be very close to it. Among the 17 measured RDCs, C–H vectors of C3 and C5 are nearest to the C4 center. The differences of calculated and measured RDCs C3–H3, C5–H5 $\alpha$ , and C5–H5 $\beta$  are also shown in Figure 5C,D for isomer 14 and its C4-diastereomer isomer 16, respectively. The configuration of C3–H3 is fixed (*cis* to C2–H2) by chemical necessity, and it is not sensitive to the configurations of its neighbors. If all three neighboring C–H vectors are removed from the calculation of the overall rmsd, then the two diastereomers (isomer 14 and isomer 16) have very similar average rmsd's (0.35 and 0.28, respectively), while the average rmsd of these three key points is 0.62 and 1.16, respectively. For C5–H5 $\alpha$  and C5–H5 $\beta$  only, the difference of the average rmsd of isomer 14 (0.69) and isomer 16 (1.40) is even greater, while the difference for the remaining 15 points is only 0.05.

To distinguish isomer 14 from isomer 16, the average rmsd difference of 0.55 and 0.41 is of course insufficient, but the difference of 1.26–0.42 Hz for the C5–H5 $\beta$  vector, as well as

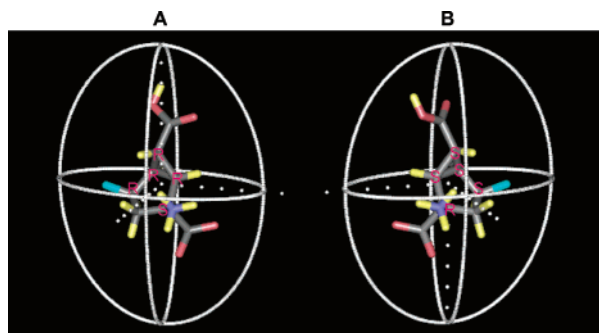


**Figure 6.** Orientations of isomer 14 (A) and isomer 3 (B) of compound **1** in the laboratory frame. The white dotted lines indicate the principal axis of the molecular order tensors, and the orientation halos are presented by the white curves.

**Table 3.** Orientation Tensor Parameters of Isomer 3 and Isomer 14 of Compound **1** Resulting from the Order Matrix Calculation

parameter	aligned by the phage		aligned by the bicelles	
	isomer 3	isomer 14	isomer 3	isomer 14
rmsd	0.21	0.21	0.42	0.41
$D_a$	$-5.62 \times 10^{-5}$	$-5.62 \times 10^{-5}$	$-2.06 \times 10^{-4}$	$-2.06 \times 10^{-4}$
$D_r$	$-1.20 \times 10^{-5}$	$-1.20 \times 10^{-5}$	$-5.21 \times 10^{-5}$	$-5.22 \times 10^{-5}$
$\alpha$	122.6	69.6	119.0	72.8
$\beta$	-68.3	26.3	-79.2	36.9
$\gamma$	-26.8	-16.5	-48.1	-39.6
$S_{zz}$	$3.80 \times 10^{-5}$	$3.81 \times 10^{-5}$	$1.28 \times 10^{-4}$	$1.28 \times 10^{-4}$
$S_{yy}$	$7.44 \times 10^{-5}$	$7.42 \times 10^{-5}$	$2.85 \times 10^{-4}$	$2.85 \times 10^{-4}$
$S_{xx}$	$-1.12 \times 10^{-4}$	$-1.12 \times 10^{-4}$	$-4.13 \times 10^{-4}$	$-4.13 \times 10^{-4}$

1.53–0.88 Hz for C5–H5 $\alpha$ , gives us good indication as to the configuration at C4. Isomer 14 is the final solution from one pair of C4-diastereomers, isomer 14 and isomer 16. Its enantiomer (isomer 3) is another indistinguishable conclusion from the analysis of another pair of C4-diastereomers, isomer 1 and isomer 3. Therefore the relative stereochemistry of all five stereocenters of this organic compound was determined unambiguously using RDCs only; the chiral configurations at five centers are 1*R*2*R*3*R*4*S*6*R* (isomer 14) or 1*S*2*S*3*S*4*R*6*S* (isomer 3). The orientations of isomer 3 and isomer 14 in the laboratory frame are shown along with their order tensor halos in Figure 6, and the order tensor parameters are presented in Table 3. The order matrix calculation outputs the same axial and rhombic components for the two enantiomers and therefore results in the same principle alignment frame ( $S_{zz}$ ,  $S_{yy}$ , and  $S_{xx}$ ) from eq 2. In summary, the molecular order tensors of these two enantiomers are also mirror images. The same order matrix analysis was carried out based on the RDC data of the phage sample and yielded the same result as obtained with the bicelle data.

We cannot distinguish enantiomers in our systems. Although the phage is chiral, we are not exploiting that property in this RDC analysis. To determine the absolute stereochemistry, a chiral reference is necessary. In practice, some information can usually be tracked from the synthetic route. In this specific case, the configuration of C3 is constrained to the *R* configuration from the known stereochemistry of the starting material.<sup>44</sup> Therefore, the absolute stereochemistry of compound **1** was solved formally by RDC and that is isomer 14 with the configurations of 1*R*2*R*3*R*4*S*6*R*.

**Crystallographic Study of Compound 1.** Compound **1** was crystallized by evaporation from a water solution at room temperature. Its absolute structure was previously determined

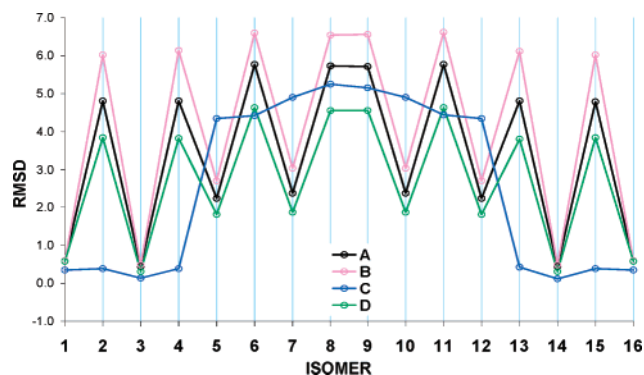


**Figure 7.** Plots of the average rmsd of calculated and measured RDCs vs isomer. (A, black): Calculation was performed with 17 measured RDCs, as listed in Table 2. (B, pink): Calculation was performed with nine measured C–H and H–H RDCs, as listed in Table 2. (C, blue): Calculation was performed with only six measured C–H RDCs, as listed in Table 2. (D, green): Calculation was performed with 17 measured RDCs, as listed in Table 2, as well as additional 15 predicted RDCs obtained on the basis of the orientation tensor and the structure of isomer 14. To distinguish isomer 14 and its diastereomer isomer 16, one C–N, one C–C, nine C–H, and four N–H RDCs which are related to the center C4 were calculated.

by relating the stereochemistry of the fluorinated carbon to that of the known stereocenter of L-alanine in the chiral derivative (US Patent 5,958,960) using standard techniques.<sup>45</sup> Molecule **1** crystallizes with the five-membered ring adopting an envelope (E) conformation with C5 displaced endo with respect to the three-membered ring. The compound is zwitterionic, with C8 existing as the carboxylate ion and C7 in the carboxylic acid form. The C7 carboxylic acid group is nearly orthogonal to the plane subtended by C2C3C6, having a C3–C6–C7–O7 torsion angle of 157.6°. There were no unusual features regarding the crystallographic structure of compound **1**.

**Order Matrix Calculation for Small Molecules** The model compound has a fluorine in the structure; therefore  $^{13}\text{C}$ – $^{19}\text{F}$  and  $^1\text{H}$ – $^{19}\text{F}$  RDCs were measured in addition to  $^{13}\text{C}$ – $^1\text{H}$  and  $^1\text{H}$ – $^1\text{H}$  RDCs. However not all investigated organic molecules have measurable  $^{13}\text{C}$ – $^{19}\text{F}$  or  $^{19}\text{F}$ – $^1\text{H}$  RDCs. The calculation was also performed with only nine  $^{13}\text{C}$ – $^1\text{H}$  and  $^1\text{H}$ – $^1\text{H}$  RDCs obtained by 1D HMQC and 1D proton experiments. The result (Figure 7B, pink) is basically the same as that obtained with all 17 RDCs including six  $^{13}\text{C}$ – $^{19}\text{F}$  and two  $^1\text{H}$ – $^{19}\text{F}$  RDCs (Figure 7A, black). Isomers 14 and 3 have the smallest rmsd of all 16 isomers. Twelve isomers were removed by rmsd analysis, and four isomers (two pairs of enantiomers or two pairs of C4-diastereomers) could not be distinguished using the overall rmsd for the entire molecule only. Even the rmsd differences between isomer 14 and isomer 16, as shown in Table 4 (calculations 2 and 4), are very close. There is no doubt that the presented methodology using RDC only to determine stereochemistry is also applicable for compounds with only measurable  $^{13}\text{C}$ – $^1\text{H}$  and  $^1\text{H}$ – $^1\text{H}$  RDCs.

In the order tensor analysis, RDCs are used to determine the five independent elements of a symmetric and traceless  $3 \times 3$  order matrix.<sup>23,24</sup> These five parameters can be reformulated in terms of an alignment of axes (three angles) for a principle order frame and values of principal order parameters ( $S_{zz}$ ,  $S_{yy}$ , and  $S_{xx}$ ). In principle, a minimum of five independent RDCs are

(45) Glusker, J. P.; Lewis, M.; Rossi, M. In *Crystal Structure Analysis for Chemists and Biochemists*; Marchand, A. P., Ed.; VCH Publishers: Weinheim, 1994; pp 573–625.



**Table 4.** Analysis of the Order Matrix Calculation for Compound 1

calc	total	description	input RDC							undistinguished <sup>f</sup>	
			av <sup>a</sup> (Hz)	max. <sup>b</sup> (Hz)	min. <sup>c</sup> (Hz)	I14 <sup>d</sup> (Hz)	I16 <sup>e</sup> (Hz)	I14 - I16  (Hz)	no.	center	
1	32	17 exp. and 15 calc. <sup>g</sup>	2.52	4.23	0.30	0.30	0.54	0.24	4	C4	
2	17	6 C-H, 6 C-F, 2 F-H, 3 H-H	4.38	5.72	0.41	0.41	0.55	0.14	4	C4	
3	12	6 C-H, C1-F, 2 F-H, 3 H-H	5.98	6.85	0.49	0.49	0.66	0.17	4	C4	
4	9	6 C-H, 3 H-H	7.02	6.57	0.48	0.48	0.62	0.14	4	C4	
5	7	6 C-H, F-H1	6.76	5.92	0.10	0.10	0.35	0.25	4	C4	
6	7	6 C-H, H1-H5 $\beta$	6.77	9.70	0.44	0.44	0.49	0.05	4	C4	
7	7	6 C-H, F-C1	7.18	5.18	0.10	0.10	0.33	0.23	8	C1, C4	
8	6	6 C-H	7.65	5.17	0.11	0.11	0.32	0.21	8	C1, C4	
9	6	5-C-H, H1-H5 $\beta$	7.77	6.16	0.34	0.34	0.49	0.15	12	C1, C4, C6	

<sup>a</sup> The data are averaged from the absolute values of corresponding RDCs. <sup>b</sup> Maximum value of rmsd of 16 isomers. <sup>c</sup> Minimum value of rmsd of 16 isomers. <sup>d</sup> I14 = isomer 14 <sup>e</sup> I16 = isomer 16 <sup>f</sup> Number of the isomers that cannot be distinguished from isomer 14 using rmsd value only. Isomer 14 is included. <sup>g</sup> 17 experimentally measured RDCs are listed in Table 1; 15 predicted RDCs were calculated from the structure and orientation tensor of isomer 14, including one C-N RDC (C4-N1), one C-C (C4-C8), nine C-H (C4-H1, C4-H3, C4-H5 $\alpha$ , C4-H5 $\beta$ , C4-H6, C8-H3, C8-H5 $\alpha$ , C8-H5 $\beta$ , and C8-H6), and four N-H (N-H3, N-H5 $\alpha$ , N-H5 $\beta$ , and N-H6).

necessary for the calculation, but typically 10 and more RDCs are required for the order matrix analysis.<sup>28,29,31</sup> If only six <sup>13</sup>C-<sup>1</sup>H RDCs are used, the resultant calculation, as shown in Figure 7C (blue line) and calculation 4 in Table 4, is different from that obtained with 17 RDCs. Although isomer 14 has the smallest rmsd, only 8 isomers (instead of 12) can be eliminated using the average rmsd. In addition to the C4-diastereomer (isomer 16) of isomer 14, the undistinguished isomers are isomer 14's C1-diastereomer (isomer 15) and its C4-diastereomer (isomer 13) as well as their enantiomers (isomers 1, 2, 3, and 4). If one more <sup>1</sup>H-<sup>1</sup>H RDC related to the C1 center is added into the calculation, a result similar to calculation 2 in Table 4 (also in Figure 4 and black line in Figure 7) was obtained (calculation 5 or 6 in Table 4). But the addition of the F-C1 RDC did not help to narrow the screening, as shown by calculation 7 in Table 4. For this specific compound, the minimum number of RDCs to run the simulation is six. Another example using six RDCs is shown by calculation 9 in Table 4 obtained with C1-H1, C2-H2, C3-H3, C4-H4, C5-H5 $\beta$ , and H1-H5 $\beta$  RDCs. Although the calculation was carried out, the rmsd could only narrow the screening from 16 to 12 isomers. When the number of input RDCs was reduced to five, the calculation yielded an unreasonable result for every isomer. The unreasonableness arises from the fact that the tensor perfectly fits those five input couplings, but cannot accurately predict the couplings not included in the input set of couplings.

To see if a larger distinction between crystal structure (isomer 14) and its C4-diastereomer (isomer 16) could be obtained, <sup>13</sup>C-<sup>13</sup>C, <sup>13</sup>C-<sup>15</sup>N, and long-range <sup>13</sup>C-<sup>1</sup>H and <sup>15</sup>N-<sup>1</sup>H RDCs related to the C4 center were calculated from the known order tensor and the structure of isomer 14. The predicted RDCs were then put into the input RDC table for the calculation. Under the assumption that all these RDCs are accurately measured and no measurement deviation is considered, the rmsd difference between the two C4-diastereomers, isomer 14 and isomer 16, increases from 0.14 to 0.24 Hz, as shown by calculations 2 and 1, respectively. The calculation result is also presented in Figure 7. The result obtained with 32 RDCs (Figure 7D, green) is basically the same as that obtained with 17 measured RDCs (Figure 7A, black) and that obtained with only nine <sup>13</sup>C-<sup>1</sup>H and <sup>1</sup>H-<sup>1</sup>H RDCs (Figure 7B, pink). The additional predicted RDCs still could not adequately distinguish isomer 14 and isomer 16, because their values are very small. All 15 calculated RDCs (one-bond <sup>13</sup>C-<sup>13</sup>C and <sup>13</sup>C-<sup>15</sup>N, long-range <sup>13</sup>C-<sup>1</sup>H

and <sup>15</sup>N-<sup>1</sup>H) are less than 1 Hz except that of two-bond C4-H5 $\alpha$ , which is 1.35 Hz. As indicated by eq 1, not all vectors are equally sensitive to the alignment. With the same alignment angles (both  $\theta$  and  $\varphi$ ), the short-range or through-space long-range <sup>1</sup>H-<sup>1</sup>H/<sup>19</sup>F-<sup>1</sup>H couplings are larger than the one-bond <sup>13</sup>C-<sup>1</sup>H/<sup>13</sup>C-<sup>19</sup>F RDCs due to the larger  $\gamma$  for <sup>1</sup>H and <sup>19</sup>F relative to <sup>13</sup>C. In addition, when the RDC value is small, the relative measurement error will be large and will result in large deviation in the tensor matrix calculation. This was investigated in our RDC measurements (Table 2). In fact, among the 17 measured RDCs the <sup>13</sup>C-<sup>1</sup>H and <sup>1</sup>H-<sup>1</sup>H RDCs are those that have the largest values and also cover all stereocenters. Five out of eight fluorine RDCs are long-range <sup>19</sup>F-<sup>13</sup>C RDCs; their values are smaller than 1 Hz. Comparing calculation 2 and calculation 3 in Table 4, we know that these five long-range <sup>19</sup>F-<sup>13</sup>C RDCs, including the C4-F which is the only RDC that reports the C4 center, have little effect on the order matrix calculation. Therefore, under natural abundance conditions, we do not have to perform time-consuming experiments to measure <sup>13</sup>C-<sup>13</sup>C, <sup>13</sup>C-<sup>15</sup>N, or long range <sup>13</sup>C-<sup>1</sup>H RDCs unless it is really necessary. <sup>1</sup>H-<sup>1</sup>H and one-bond <sup>13</sup>C-<sup>1</sup>H RDCs, which are the easiest to measure, are the most important data for the structural calculation of organic molecules.

The calculations listed in Table 4 also indicate that not all RDCs are equally important to the structural determination; it is structure-dependent. Among the five stereocenters of compound **1** (C1, C2, C3, C4, and C6), the configuration on C4 is the most difficult to determine using the method presented here. The lack of a proton on C4 results in an inadequate supply of RDC information directly related to this center. It is not easy to distinguish the C4 diastereomers under the conditions of insufficient RDC data because the size similarity of two substituents at C4 (-NH<sub>3</sub><sup>+</sup> and -COO<sup>-</sup>) makes the calculation difficult. Therefore, every pair of C4-diastereomers has very similar rmsd values. The second toughest center is C1. As shown by the calculations 6 and 7 in Table 4 and Figure 7C, when fewer RDC data were input, the number of undistinguished isomers increased from four to eight, and this increase is due to the four isomers related to the C1 center. C1 has two measurable vectors, <sup>13</sup>C-<sup>1</sup>H and <sup>13</sup>C-<sup>19</sup>F. Since H and F have similar atomic radius, additional information about the relationship of these two atoms (calculation 5 in Table 4) or the relationship of this center to the others (calculation 6 in Table 4) is necessary to determine the C1 configuration. The size



difference of H and  $-\text{COOH}$  at C6 makes the *R* and *S* configurations at this center easier to distinguish than those at C1 or C4. Due to strain constraints of the fused ring, the chiralities of C2 and C3 are the same. The change of the configurations at C2 and C3 will introduce a flip of the fused ring and result in a tremendous conformational change of the entire molecule. The stereochemistry determination of the C2 and C3 centers is the easiest for this compound. In any case in Table 4, isomer 14 has the smallest rmsd among the 16 isomers, and the result is in agreement with the crystallographic study. The presented methodology is therefore a powerful technique for the determination of stereochemistry for the organic compounds.

## Conclusion

In combination with the order matrix calculation, RDCs were used to unambiguously solve the complete relative stereochemistry of an organic molecule. The investigated molecule is a low molecular weight compound with five stereocenters. The number of potential chiral isomers is 16.  $^{13}\text{C}-^1\text{H}$ ,  $^{13}\text{C}-^{19}\text{F}$ ,  $^{19}\text{F}-^1\text{H}$ , and  $^1\text{H}-^1\text{H}$  RDCs were measured using three one-dimensional experiments. The order matrix analysis was performed on each isomer independently. The fits were evaluated by the rmsd of calculated and measured RDCs. Analysis of rmsd's narrowed the candidates from 16 to four isomers. Further analysis of the output data point-by-point reduced the four isomers to two, which are enantiomers. Therefore the complete relative stereochemistry of this compound was solved using RDC only. The order tensor simulations based on two different sets of RDC data collected with phage and bicelles yielded consistent results. But the use of bicelles as an alignment media is preferred since a larger magnitude of RDC was obtained using only one single sample. The single crystal of this compound was also obtained, and its structure was studied by X-ray diffraction analysis. The result obtained from only RDC is in perfect agreement with the X-ray crystallographic study.

In principle, a minimum of five independent RDCs are necessary as input for the order matrix calculation to solve the five independent elements of a symmetric and traceless  $3 \times 3$  order matrix.<sup>23,24</sup> For this specific compound, six RDCs are necessary to run the calculation and seven are the minimum to get an acceptable result. On the other hand, nine  $^{13}\text{C}-^1\text{H}$  and  $^1\text{H}-^1\text{H}$  RDCs provide basically the same result as 17 or even 32 RDCs, because most of the additional RDCs are small magnitude data with significant errors. It is shown that  $^{13}\text{C}-^1\text{H}$  and  $^1\text{H}-^1\text{H}$  RDCs, which are the easiest to determine, are the most important data for the order matrix calculation. When dealing with molecules that are not isotopically labeled, it is not necessary to work on the time-consuming experiments to measure small magnitude RDC data, such as  $^{13}\text{C}-^{13}\text{C}$  or long-range  $^{13}\text{C}-^1\text{H}$  RDCs, which do not add precision to the calculation. The effect of each RDC on the calculation also depends on the location of the corresponding vector in the structure. The direct RDC information about each stereocenter is important, although not critical, to the configuration determination of this center.

RDC is a powerful technique for the determination of stereochemistry of organic molecules. A simple inspection of C-H RDCs can connect two remote stereocenters and provide accurate information about the relative orientations of some

types of compounds, such as six-membered chair compounds.<sup>27</sup> When the order matrix calculation is combined, the complete relative stereochemistry of all stereocenters within a molecule can be determined simultaneously and unambiguously. The configuration of the stereocenter without proton can also be concluded. Since only around 10 one-bond C-H, short-range or through-space, long-range H-H and other easy-to-be-measured RDCs are necessary for the structural calculation, the presented methodology has potential widespread application in structural studies of organic molecules and natural products. One caveat is that enantiomers cannot be distinguished by this method alone, but in conjunction with chemical knowledge of the starting materials, enantiomers are easily distinguished. This is especially true for sample-limited situations where the quantity is insufficient for X-ray crystallographic studies.

## Experimental Section

**Materials.** Compound **1**, as shown in Scheme 1, was synthesized and purified at Eli Lilly and Company. Pf1 bacteria phage was prepared and purified as described by Hansen et al.<sup>33</sup> 1,2-Dimyristoyl-*sn*-glycero-3-phosphocholine (DMPC) and 1,2-dihexanoyl-*sn*-glycero-3-phosphocholine (DHPC) (2.8:1 molar ratio) were purchased from Avanti Polar Lipids, Inc. (Alabaster, AL).

**Phage Sample Preparation** Compound **1** was dissolved into  $1 \times$  phosphate-buffered saline (PBS) of 99.9%  $\text{D}_2\text{O}$  (pD 7.30) to yield a concentration of 250 mM. Phage pellets was resuspended and pelleted twice into 0.4 mL of PBS buffer. Isotropic and aligned samples were prepared by diluting the concentrated solution in  $1 \times$  PBS buffer and PBS resuspended phage solution, respectively. The final pD was about 8.1. The concentration of compound **1** was 10 mM. The concentration of phage was 14 mg/mL, and 12.7 Hz splitting of DOH signal was observed on the deuterium spectra.

**Bicelle Sample Preparation** The buffer used to prepare bicelle sample is 10 mM phosphate in  $\text{D}_2\text{O}$  containing 2.4 mM tetradecyltrimethylammonium bromide (TTAB) and 0.02% sodium azide ( $\text{NaN}_3$ ) with pD of 6.8. TTAB is used to increase bicelle stability. Bicelles were dissolved into filtered buffer under  $\text{N}_2$  atmosphere to yield a concentration of 15%. Bicelles were vortexed for 10 min and then left for an additional 15 min at 4 °C. After 1 min of vortexing at room temperature, the solution was kept at 38 °C for 30 min. It was cooled for 15 min and vortexed for 30 min at 4 °C, then warmed for other 15 min and vortexed for another minute at room temperature followed by 30 min at 38 °C. The process from cooling for 15 min at 4 °C to heating for 30 min at 38 °C was repeated three times. After hydration, concentrated compound **1** solution was then added and the bicelle concentration was adjusted to 10% (w/v). Compound **1** was dissolved into the buffer, and the pD was adjusted to 6.5 previously. At 4 °C, the solution was mixed by 2 min vortexing and transferred into a NMR tube followed by a light centrifugation. The transition temperature was found to be 32 °C, which was much lower than the reported value. It might result from a more effective hydrolysis of DHPC relative to DMPC as the bicelles age. Spectra of the bicelle sample were recorded at 25 and 31 °C for isotropic and oriented measurements, respectively. A DOH splitting of 10.4 Hz was obtained in the deuterium spectrum at 31 °C.

**NMR Measurements of Residual Dipolar Couplings.** All NMR experiments were performed on a Bruker Avance DRX 500 MHz spectrometer with a 5 mm inverse triple-resonance ( $^{15}\text{N}/^{13}\text{C}/^1\text{H}$ ) probe equipped with a *z* axis actively shielded gradient. The temperature was controlled by a Bruker BVT 3000. The data were processed using XwinNMR (Bruker).

The C-H scalar and dipolar couplings were measured by 1D HMQC<sup>27,43</sup> in the  $^1\text{H}$  dimension without decoupling in the acquisition period. The 1D HMQC spectra were acquired with 32k data points

over a spectrum width of 4006 Hz (8.0 ppm) and 5000 Hz (10.0 ppm) for an experimental resolution of 0.12 and 0.15 Hz per point for phage and bicelle sample, respectively. A heteronuclear transfer delay  $\tau$  of 3.25 or 3.45 ms corresponding to a  $J$  constant of 160 or 145 Hz was used. Before Fourier transformation an exponential window function with 0.6 Hz line broadening and a zero-filling by a factor of 2 were applied. The signal of each satellite was phased and frequency output independently. The  $J$  and  $J + RDC$  splittings were measured as the separation between  $^{13}\text{C}$  satellites of a given resonance. Suppression of the  $\text{H}_2\text{O}$  signal was achieved by a presaturation in the recovery period.

The C–F scalar and dipolar couplings were measured by a 1D NOE enhanced  $^{13}\text{C}$  experiment.  $^1\text{H}$  was decoupled during the recovery and acquisition periods. The C–F splittings were measured since  $^{19}\text{F}$  was not decoupled. 80k data points were used for a spectral width of 12 626 Hz (100.4 ppm), resulting in the FID resolution of 0.19 Hz. An exponential window function with 1 Hz line broadening and a zero-filling by a factor of 2 were applied before Fourier transformation.

The H–H and F–H scalar and dipolar couplings were measured using 1D proton spectra. The spectra were recorded with 32k data points to cover a spectral width of 4006 Hz (8.0 ppm) and 5000 Hz (10.0 ppm) for an experimental resolution of 0.12 and 0.15 Hz per point for phage and bicelle samples, respectively. The  $\text{H}_2\text{O}$  signal was saturated in the recovery period of 2.0 s. A zero-filling by a factor of 2 was applied before Fourier transformation, but no window function was used.

When the proton signal was investigated, the measurement was based on the average of multiplets, and the measurement deviation of multiple peaks is smaller than the FID resolution. The experiments for RDC determination were repeated two or three times.

2D DQF-COSY<sup>46</sup> experiments were recorded to assist the assignments of chemical shifts and F–H and H–H couplings. 256 × 1024 data points were used in both  $F_1$  and  $F_2$  dimensions with a sweep width of 4006 Hz (8.0 ppm). Quadrature indirect detection was achieved through TPPI. The recovery delay was 2 s. The homonuclear spectra were processed by applying a cosine<sup>2</sup> function to both dimensions prior to zero-filling by a factor of 2 before Fourier transformation. NOESY<sup>47</sup> was recorded with 2048 × 256 data points to cover a sweep width of 4808 Hz in each dimension. Quadrature indirect detection was achieved through TPPI. The mixing time was 1.2 s, and the recovery delay was 2 s. A cosine<sup>2</sup> function was applied to both dimensions prior to zero-filling by a factor of 2 before Fourier transfer.

Some broad lipid signals were observed when the bicelle sample was detected. The strong lipid signals have interference on the measurement of proton signals but not on the measurement of carbon signals. A CPMG  $T_2$ -filter<sup>48,49</sup> with a total length of 8 or 16 ms was successfully used to eliminate the lipid signals of bicelles.

**Molecular Order Tensor Matrix Calculation.** All the simulation studies were carried out on an SGI workstation. The initial structure

of each chiral isomer was built up atom-by-atom and energy-minimized using the molecular modeling program Insight II (2000, Biosym/MSI, San Diego, CA). The tensor matrix analysis was performed by NMRPipe.<sup>50</sup> In the input RDC table, all RDC measurement-related atoms except H5 $\alpha$  and H5 $\beta$  have a one-to-one relationship with the atomic coordinates of the initial structure. H5 $\alpha$  and H5 $\beta$  were defined as the protons that are on the same side and on the inverse side of H6 on the fused ring, respectively. The input RDCs were weighted by a  $w$  factor, which depends on the measurement uncertainty. For all H–H, F–H, and other one-bond C–H, C–F couplings, the  $w$  factor was set to 1 if the measurement error (Table 1) is smaller than  $2 \times \text{FID-resolution}$ . Otherwise it was 0.1. The calculation was performed for each of the 16 isomers independently. The orientation tensor of each isomer was simulated using single-value decomposition.<sup>24</sup> The orientation of the molecule in the laboratory frame is described by the output axial and rhombic components  $D_a$  and  $D_r$  as well as Euler angles  $\alpha$ ,  $\beta$ , and  $\gamma$ . The order matrix parameters  $S_{nm}$  ( $n = x, y, \text{ or } z$ ) are reformulated<sup>25</sup> and reported. With the molecular order tensor, the RDC of any vector can be predicted from a given structure. Fits were evaluated using the root-mean-square deviation of calculated and measured RDCs, as shown in eq 3.

**Single-Crystal Diffraction Analysis.** High-quality crystals of were grown by slow evaporation from water. A single crystal ( $0.11 \times 0.26 \times 0.42$  mm) was mounted on a thin glass fiber and immersed in a stream of nitrogen at  $-173$  °C. Data were collected using a Mo  $K\alpha$  radiation source ( $\lambda = 0.71073$  Å) and a P4 diffractometer equipped with a SMART 1000 CCD area detector (Siemens Industrial Automation, Inc., Madison, WI). Cell refinement and data reduction were performed using the SAINT program. The unit cell was indexed, having monoclinic cell parameters of  $a = 20.065(11)$  Å,  $b = 5.741(3)$  Å,  $c = 7.394(4)$  Å, and  $\beta = 96.042(10)^\circ$ . The cell volume of  $847.0(8)$  Å<sup>3</sup> and density of  $1.593$  g/cm<sup>3</sup> suggested four molecules in the unit cell. The systematic absences were consistent with the chiral space group  $C_2$ . The structure was solved by direct methods.<sup>51</sup> All atomic parameters were independently refined. The space group choice was confirmed by successful convergence of the full-matrix least-squares refinement on  $F^2$ . The final residual factors,  $R_1 = 0.0504$  and  $wR_2 = 0.0840$ , with the largest difference peak and hole after the final refinement cycle were 0.481 and  $-0.389$  ( $e \cdot \text{Å}^{-3}$ ), respectively.

**Supporting Information Available:** X-ray crystallographic file in CIF format. This material is available free of charge via the Internet at <http://pubs.acs.org>.

JA037605Q

(46) Derome, A.; Williamson, M. *J. Magn. Reson.* **1990**, *88*, 177–185.

(47) Jeener, J.; Meier, B. H.; Bachmann, P.; Ernst, R. R. *J. Chem. Phys.* **1979**, *71*, 4546–4553.

(48) Meiboom, S.; Gill, D. *Rev. Sci. Instrum.* **1958**, *29*, 688–691.

(49) Carr, H. Y.; Purcell, E. M. *Phys. Rev.* **1954**, *94*, 630–638.

(50) Delaglio, F.; Grzesiek, S.; Vuister, G. W.; Zhu, G.; Pfeifer, J.; Bax, A. *J. Biol. NMR* **1995**, *6*, 277–293.

(51) Sheldrick, G. M. *Acta Crystallogr., Sect. A* **1990**, *46*, 467–473.